

# Deriving plasticity: Burgers equation, Landau theory, and irreversibility

James P. Sethna\* and Markus Rauscher†

*Laboratory of Atomic and Solid State Physics (LASSP),*

*Clark Hall, Cornell University, Ithaca, NY 14853-2501, USA*

Jean-Philippe Bouchaud‡

*Service de Physique de l'Etat Condensé,*

*CEA Saclay, 91191 Gif sur Yvette, France*

(Dated: December 2, 2024)

## Abstract

We expand the most general scalar theory for rate-independent plasticity allowed by symmetry. We find that a special case of this theory forms an anisotropic Burgers equation which forms shock fronts at finite times. We show that these shocks introduce the same irreversibility seen in real plasticity: our model exhibits yield stress, work hardening, reversibility under unloading, and cell boundary formation, giving realistic stress-strain curves.

PACS numbers: 46.35.+z, 62.20.Fe, 83.60.La

Keywords: plasticity, yield stress, cell formation, strain gradient theory

The field of multiscale modeling is attempting to explain the macroscopic deformation and failure of structural materials starting from quantum mechanics. Physicists know in principle how to go from quantum mechanics up to the motion and interaction of dislocations, and engineers have a useful description of the macroscale behavior, but between these scales, there is an enormous gap. In particular, we do not understand quantitatively the striking structures and patterns formed by dislocations on intermediate micron scales. The field needs an intermediate mesoscale description for the effective laws emerging from the interactions between the microscopic defects in materials.

We call it plasticity when materials yield irreversibly at large external stresses. Macroscopically, plasticity is associated with three qualitative phenomena. To a good approximation, there is a threshold called the *yield stress* below which the deformation is reversible (see Fig. 1). A material pushed beyond its yield stress exhibits *work hardening*, through which the yield stress increases to match the maximum applied stress. Finally, at large deformations ( $\approx 25\%$ ) the deformed crystal develops patterns, such as the *cell structures* observed in fcc metals<sup>1,2,3</sup>. While much is known about all three phenomena, our engineering colleagues suggest that a quantitative understanding based on systematic theory would be welcome – especially if it connects to microscopic properties of the atomic interactions in the material. In this paper, we will present a simple continuum model which naturally exhibits these three key features of plasticity. Our model clearly is not complete, but we think that a continuum theory of plasticity has to be in the same family: in particular, we believe the finite time singularities in our theory may be generic for continuum theories of rate-independent plasticity.

There are many existing continuum theories of plasticity. (1) There are those based on the differential geometry and the Burgers vector density torsion tensor<sup>4</sup>, which ignore the geometrically unnecessary dislocations which dominate the work hardening. (2) There are the  $J_2$  theories incorporating work hardening by hand, and generalizations including slip systems<sup>5</sup> and strain gradients<sup>6</sup>, which are appropriate for scales large compared to the cell-boundary structures we describe. (One should note, however, that Mika & Dawson<sup>5</sup> use this approach in a polycrystal, and find cell-like structures emerging.) (3) There are reaction-diffusion systems<sup>7,8</sup> which incorporate immobile dislocations to get irreversibility, and exhibit pattern formation reminiscent of slip bands. (4) There are theories which are based on approximate descriptions of the microscopic behavior<sup>9,10,11</sup>; these theories show

both pattern formation and features of irreversibility. (5) There are theories which appear to develop fractal cell-boundary structures<sup>9,12,13</sup>. (6) There are microstructure theories based on nonconvex minimization problems,<sup>14</sup> which incorporate in full detail the compatibility of the geometry but for which the dynamical evolution law is assumed to stem from a variational principle. None of these theories provide explanations for the observed yield stress and work hardening phenomenology: they either do not address it or they incorporate it explicitly.

Our theory is in the tradition of Landau theory: we write the most general analytic theory for a scalar order parameter  $\Psi$  allowed by symmetry for an isotropic material. We use a scalar order parameter for simplicity: plasticity is far from equilibrium, so there is likely no finite-dimensional local order parameter which captures the dislocation structure completely.  $\Psi$  can represent, any scalar property of the material which tracks the work hardening and plastic deformation. We assume analyticity in the evolution equations as is traditional in physics: one must note that, unlike equilibrium statistical mechanics, we have no microscopic justification for assuming that the theory involves integer powers of  $\Psi$  and its gradients. We assume a local theory, ignoring the long range interactions<sup>9</sup> and the line like nature of dislocations<sup>4</sup>. We assume, as do the engineers, that the evolution depends only on the deviatoric stress  $S_{ij} = \sigma_{ij} - \frac{1}{3}\sigma_{kk}\delta_{ij}$  (*i.e.* not on volume changes). We focus, as is traditional, on rate-independent plasticity, ignoring inertia and creep (although the latter is effectively included numerically, see below), so our evolution law up to first order in  $S_{ij}$ , and second order in gradients is

$$\frac{\partial \Psi}{\partial t} = g \frac{\partial S_{ij}}{\partial t} \nabla_i \nabla_j \Psi + h \frac{\partial S_{ij}}{\partial t} \nabla_i \Psi \nabla_j \Psi, \quad (1)$$

where  $g$  and  $h$  are material-dependent parameters whose dependence on  $\Psi$  we ignore for convenience. We will focus on proportional loading paths (such as those used in shear and tension tests) where the stress  $S_{ij}(t) = \sigma(t) \hat{S}_{ij}$ , in which case we may change variables from time  $t$  to stress amplitude  $\sigma$ :

$$\frac{\partial \Psi}{\partial \sigma} = g \hat{S}_{ij} \nabla_i \nabla_j \Psi + h \hat{S}_{ij} \nabla_i \Psi \nabla_j \Psi. \quad (2)$$

In the form of Eq. (2), we see the key challenge in writing laws of rate-independent plasticity: the equations appear manifestly reversible. Increasing and then reducing  $\sigma$  will leave the material in the original state. Indeed, an arbitrary curved path in strain space  $S_{ij}(t)$  when reversed along the same path will naively return to the original state. The

engineers bypass this problem by formulating their theories not in terms of order parameter fields, but directly in terms of a yield surface (corresponding to step functions  $\Theta(\sigma - \sigma_y)$  in the equations of motion).

The second term on the right, multiplied by  $h$ , is the source of irreversibility. It gives a multidimensional anisotropic Burgers equation<sup>15</sup>, which develops shock singularities at finite time. At these singularities, as numerically illustrated below, information is lost. The yield stress where reversibility is lost is the point where the first singularities form.

The first term on the right is diffusion-like, but because  $S_{ij}$  is traceless this term necessarily has some directions in which the diffusion constant is negative. This antidiffusion term poses important conceptual and numerical difficulties, and we have dropped it. One possible justification is the limit where the antidiffusion term  $g d\sigma/dt$  is smaller than  $D$  in a rate-dependent creep term  $D\nabla^2\Psi$  for Eq. (1). This is true if the agglomerative antidiffusive motion induced by shear during the experiment is smaller than the random diffusion induced by thermal creep. Although the creep diffusion term does not appear explicitly in our equations, it is effectively incorporated in our numerics as a regularization which is proven to yield the so-called “viscosity solution” that we have chosen. We will return to discuss antidiffusion in the conclusion.

We solve Eq. (2) numerically on a finite difference grid using the problem solving environment CACTUS 4.0<sup>17</sup>. The initial condition was a Gaussian random field. The convolution was performed in Fourier space using the fast Fourier transform package FFTW 2.1.3<sup>18</sup>. We use an essentially nonoscillatory (ENO) scheme in combination with Godunov’s method to minimize numerical damping<sup>19</sup>. The algorithm is proven to converge to the viscosity solution. The numerical grid has periodic boundary conditions; in one dimension the length of the system is 100 and the system had 4084 points; in two dimensions the size of the system is  $25^2$  and the grid was  $1016^2$ . The three dimensional simulation cell was  $12.5^3$  and the grid size  $264^3$ . The ENO stencil width was 4 in one and 5 in two and three dimensions, respectively, and the time stepping scheme is a simple explicit Euler scheme with a time step  $\delta\sigma = 10^{-3}$ . The system is cycled by unloading beginning at various points  $\sigma_n$  and reloading at somewhat above zero stress (to reduce the effect of numerical damping).

Fig. 2 shows the evolution of the Burgers equation in one dimension, corresponding to Eq. (2) with  $h = 1/2$ ,  $S_{ij} = 1$  and  $g = 0$ . The cusps develop in the valleys at  $\sigma \approx 0.3$ , and the unloading and reloading paths are both shown. Since the cusps disappear immediately

upon unloading, the order parameter evolution is reversible until the stress grows to match the previous maximum, so our model exhibits work hardening.

Finally, Fig. 3 shows the shock locations in two two-dimensional cuts of the three-dimensional simulation with  $\hat{S}_{xx} = 2/3$ ,  $\hat{S}_{yy} = \hat{S}_{zz} = -1/3$ , and  $\hat{S}$  zero otherwise, appropriate to a tension test. We see that the shocks form nearly flat one-dimensional interfaces separating cell-like volumes. While the cut parallel to the loading direction (a) shows the expected asymmetry, the cut perpendicular to the loading direction shows an isotropic hexagonal cell structure. Simulations under shear in two dimensions ( $\hat{S}_{xx} = 1/2$ ,  $\hat{S}_{yy} = -1/2$ , and zero otherwise) show similar shocks to Fig. 3(a). These morphologies are reminiscent of cell structures formed in hardened fcc metals<sup>1</sup>. Thus our evolution law possesses all three of the key mysterious features of plasticity.

We note here that experimental cell structures refine under increased deformation, corresponding to the distance between cell walls decreasing as  $\sigma$  increases<sup>1</sup>. Our model does not, however, refine in this way: in one dimension, Burgers equation is known to coarsen, with the distance between shocks increasing as  $\sigma^{1/2}$ . We return to this question in the conclusion.

We now wish to generate a stress-strain relation from our order parameter field. Without a microscopic picture of what  $\Psi$  represents, we can again fall back on general symmetry considerations. We assume, as do the engineers, that the deformation is in the direction of the applied stress  $S_{ij}$ . To second order in  $S_{ij}$ , and fourth order in gradients we have the spatial average of the strain

$$\left\langle \frac{\partial \varepsilon_{ij}}{\partial t} \right\rangle = \left\langle S_{ij} \frac{\partial S_{k\ell}}{\partial t} (\nabla_k \Psi) (\nabla_\ell \Psi) (A + B \nabla^2 \Psi) \right\rangle, \quad (3)$$

where the angle brackets represent spatial averages. Here we have again ignored the dependence of constants on  $\Psi$  for convenience: we then remove terms that are total derivatives (and hence integrate to zero with periodic boundary conditions). We also dropped a highly singular term  $S_{ij} \frac{\partial S_{k\ell}}{\partial t} (\nabla_k \nabla_\ell \Psi) \nabla^2 \Psi$  as it would depend upon our numerical implementation at the grid spacing. As usual, the plastic strain does not satisfy the incompatibility condition. In the spirit of Reuss models, we've assumed constant stress and ignored the elastic components of the strain; in a more complete calculation the latter will make the stress non-uniform and make the total strain compatible with a single-valued displacement field.

In Fig. 1 the elastic curves on backtracking have higher slopes than the work hardening curves. Naively, since the derivative  $\partial \varepsilon_{ij} / \partial \sigma$  is dependent only on the current  $\Psi$  field, it

would seem that any analytic expansion could not have this property. The interplay of the singularities with the term with four gradients in Eq. (3) gives us the required kink (which is why we kept four gradients). In fact, the spatial average of this term is proportional to the time derivative of the spatial average of  $(\nabla\Psi)^2$ , which can be shown to be zero in the absence of cusps in one and two dimensions: thus the term proportional to  $B$  contributes smooth plastic curves on loading and vertical reversible unloading curves.

Fig. 4 shows the resulting stress-strain curves for our plasticity theory. Notice the similarities with Fig. 1: work hardening and yield stress, and even fairly realistic stress-strain laws, seem to follow naturally using our general symmetry-based approach.

We notice under rolling in two dimensions that the term proportional to  $A$  in systems with many grains and isotropic initial conditions will average to zero, so the curvature and tilts of the unloading paths in Fig. 4 are finite-size effects. Experimentally the unloading paths are found to be predominantly linear elastic deformation (ignored in our analysis), so the vertical unloading curves are expected. In our three dimensional tension test (not shown here), the unloading curves become slightly tilted and curved as the stress increases.

We conclude by mentioning five areas for further work. The first three have been mentioned already in the text. (1) Cell structures experimentally refine, where in our model they coarsen. (2) We have not incorporated an antidiffusion term allowed by symmetry. We note that the thermal creep, mentioned as a possible remedy to antidiffusion, will disappear at low temperatures: this could conceivably be related to a brittle-ductile transition in our model if the instability implied by antidiffusion leads to fracture. Alternatively, this problem could be related to the first one: incorporating a suitably regularized antidiffusion term could amplify small initial fluctuations into large order parameter variations that the Burgers term could sharpen into new cell walls. (3) Our theory so far does not incorporate elastic strains. Incorporating inhomogeneous elastic deformations responding to the inhomogeneous plastic deformation will lead to a spatially varying stress  $S_{ij}(x)$  in Eq. (3). A complete treatment of this problem may need to incorporate stress gradients and the total derivative terms.

(4) We need some kind of microscopic picture to associate with the shock formation. It is common in physics to derive laws phenomenologically from symmetry, as we have, and only later to understand the origin of the order parameter fields: superconductors and superfluids, liquid crystals and other exotic phases were understood phenomenologically before they were

understood microscopically. We are optimistic that the microphysics of plasticity is already sufficiently well understood that we may soon have a crude picture of how the coarse-grained theory emerges. While the emergent theory may not be our anisotropic Burgers equation, we predict that it will develop singularities at finite time, and the singularities will be associated with cell walls.

(5) The physics of dislocation tangle evolution within the cell walls, in our current implementation, is subsumed under our choice of the traditional “viscosity solution” among an infinite family of possible weak solutions to the differential equation. Even if our evolution law is correct without modification away from the singularities, understanding the physics inside the cell wall will be important to picking the correct weak solution. (Creep, especially in the walls, needn’t be a simple diffusive process.) It seems likely that the evolution within the cell walls may involve rearrangement events of many scales<sup>16,20</sup>, yielding a highly non-trivial dynamics at the shock fronts.

Thus the simplest plausible theory of scalar, rate-independent plasticity appears to show quite reasonable physical behavior. The behavior is not immediately apparent in the equations, which naively are reversible and show no slope change when shifted between loading and unloading. Indeed, it is the formation of shock singularities at finite times which yield the irreversibility. The yield stress is associated with the formation of the initial shock. Work hardening is associated with the smoothening of shocks upon unloading, leading to irreversible behavior only upon reloading to the previous maximum stress. The shocks form walls which may be related to cell walls formed by plastic strain in fcc metals.

### Acknowledgments

Thanks to A. S. Argon, P. R. Dawson, D. A. Hughes, D. S. Fisher, J. Hutchinson, C. R. Myers, and M. P. Miller, for fruitful conversations. Thanks to G. Heber and W. Benger for helping with CACTUS on MS-Windows. This work was supported by the Cornell Center for Materials Research (CCMR), a Materials Research Science and Engineering Center of the NSF (DMR-0079992), by NSF KDI-9873214 and NSF ACI-0085969, and by Microsoft. We used the resources of the Cornell Theory Center, which receives funding from Cornell University, New York State, federal agencies, and corporate partners, as well as research

infrastructure support through NSF 9972853.

---

- \* Corresponding author, Electronic address: [sethna@lassp.cornell.edu](mailto:sethna@lassp.cornell.edu); URL: <http://www.lassp.cornell.edu/sethna/sethna.html>
- † Current address: Max-Planck-Institute für Metallforschung, Heisenbergstr. 1, 70569 Stuttgart, Germany; Electronic address: [rauscher@mf.mpg.de](mailto:rauscher@mf.mpg.de)
- ‡ Electronic address: [bouchau@saclay.cea.fr](mailto:bouchau@saclay.cea.fr)

- <sup>1</sup> Hughes, D. A. & Hansen, N. Scaling of Misorientation Angle Distributions. *Phys. Rev. Lett.* **81**, 4664–4667 (2001).
- <sup>2</sup> Kuhlmann-Wilsdorf, D. Theory of Plastic Deformation:-properties of low energy dislocation structures. *Mater. Sci. Eng. A* **113**, 1–41 (1989).
- <sup>3</sup> Argon, A. S. Mechanical properties of single-phase crystalline media: Deformation at low temperatures. in *Physical Metallurgy*, edited by Cahn, R. W. & Haasen, P. (North-Holland, Amsterdam, 1996), chapter 21, p. 1877–1955.
- <sup>4</sup> Rickman, J. M. & Viñals, J. Modelling of dislocation structures in materials. *Phil. Mag. A* **75**, 1251–1262 (1997).
- <sup>5</sup> Mika, D. P. & Dawson, P. R. Polycrystal plasticity modeling of intracrystalline boundary textures. *Acta. Mater.* **47**, 1355–1369 (1999).
- <sup>6</sup> Fleck, N. A. & Hutchinson, J. W. A phenomenological theory for strain gradient effects in plasticity. *J. Mech. Phys. Solids* **41**, 1825–1857 (1993).
- <sup>7</sup> Walgraef, D. & Aifantis, E. C. Dislocation patterning in fatigued metals as a result of dynamical instabilities. *J. Appl. Phys.* **58**, 688–691 (1985).
- <sup>8</sup> Glazov, M. V. & Laird, C. Size effects of dislocation patterning in fatigued metals. *Acta Metall. Mater.* **43**, 2849–2857 (1995).
- <sup>9</sup> Groma, I. & Bako, B. Dislocation patterning: From micro- to mesoscale description. *Phys. Rev. Lett.* **84**, 1487–1490 (2000).
- <sup>10</sup> Falk, M. L. and Langer, J. S., Dynamics of viscoplastic deformation in amorphous solids. *Phys. Rev. E* **57**, 7192–7205 (1998).
- <sup>11</sup> Langer, J. S., Microstructural shear localization in plastic deformation of amorphous solids. *Phys. Rev. E* **64**, 011504(1–12) (2001).

<sup>12</sup> Hähner, P., Bay, K. & Zaiser, M. Fractal Dislocation Patterning During Plastic Deformation. *Phys. Rev. Lett.* **81**, 2470–2473 (1998).

<sup>13</sup> Thomson, R. & Levine, L. E. Theory of Strain Percolation in Metals. *Phys. Rev. Lett.* **81**, 3884–3887 (1998).

<sup>14</sup> Ortiz, M. & Repetto, E. A. Nonconvex energy minimization and dislocation structures in ductile single crystals. *J. Mech. Phys. Solids* **47**, 397–462 (1999).

<sup>15</sup> Frisch, U. & Bec, J. Burgulence. in *Les Houches 2000: New Trends in Turbulence—Les Houches Session LXXIV 31 July–1 September 2000*, edited by Lesieur, M., Yaglom, A. & David, F. (Springer, 2002).

<sup>16</sup> Sethna, J. P., Dahmen, K. A. & Myers, C. R. *Crackling Noise*. *Nature* **410**, 242–250 (2001).

<sup>17</sup> <http://www.CactusCode.org>

<sup>18</sup> <http://www.fftw.org>

<sup>19</sup> Osher S. & Shu, C.-W. High-order essentially nonoscillatory schemes for hamilton-jacobi equations. *SIAM J. Numer. Anal.* **28**, 907–922 (1991).

<sup>20</sup> Miguel, M. C., Vespignani, A., Zapperi, S., Weiss, J. & Grasso, J. R. *Intermittent dislocation flow in viscoplastic deformation*. *Nature* **410**(6829), 667–671 (2001).

FIG. 1: Generic stress-strain relation. For stress  $\sigma$  below the critical yield stress  $\sigma_{y0}$  the deformation is elastic and reversible. Further deformation results in plastic deformation and work hardening, *i.e.* the yield point (bullet) moves to higher stress. The strain  $\varepsilon$  is partly due to reversible elastic deformation  $\varepsilon_e$  and partly due to irreversible plastic deformation  $\varepsilon_p$ .

FIG. 2: Blowup of the region  $18 < x < 20$  from our one-dimensional simulation. The solid lines represent  $\Psi(x)$  for  $\sigma$  values 0.1 apart starting at  $\sigma = 0$ , with curves further up having larger  $\sigma$ . The dashed lines are  $\Psi(x)$  while unloading and the dotted ones while reloading. The dotted lines are hardly visible because in the reversible region they lie on top of the dashed ones. At the cusps, the spacial discretization is visible. The inset shows the initial (solid) and final (dashed) configuration of the whole system, *i.e.* for  $\sigma = 0$  and 6.

FIG. 3: Location of the singularities for tension test at  $\sigma = 1$  in (a) the  $xy$ -plane and (b)  $yz$ -plane, that is parallel and perpendicular to the loading direction, respectively. The lines are contour lines  $\hat{S}_{ij}\nabla_i\nabla_j\Psi = 1.5, 3, 6, 9, \dots$ . Our symmetry analysis does not provide us a physical interpretation for  $\Psi$ ; two derivatives would correspond to  $\Psi$  being a kind of potential term with the net dislocation density as a source.

FIG. 4: Stress-strain relation according to Eq. (3) for our one (solid line) and two-dimensional (dashed line) model, for  $A = 0.1$ ,  $B = 1$ , and  $A = 1$ ,  $B = 1$ , respectively. The initial conditions had amplitude and correlation length one.

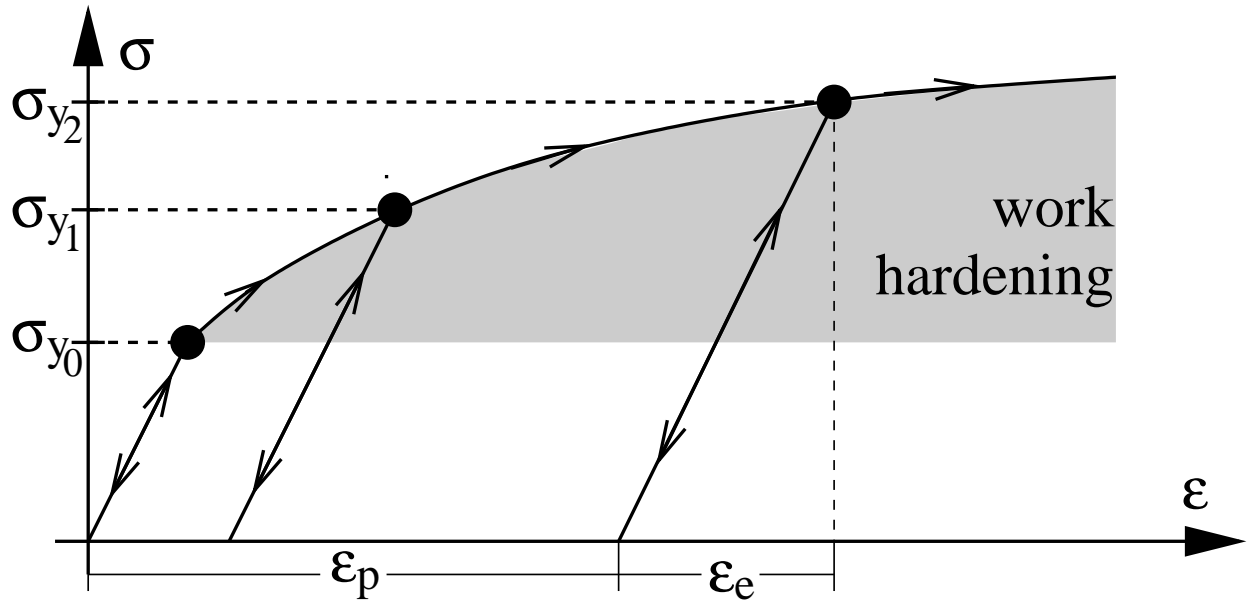


Figure 1, Sethna *et al.*

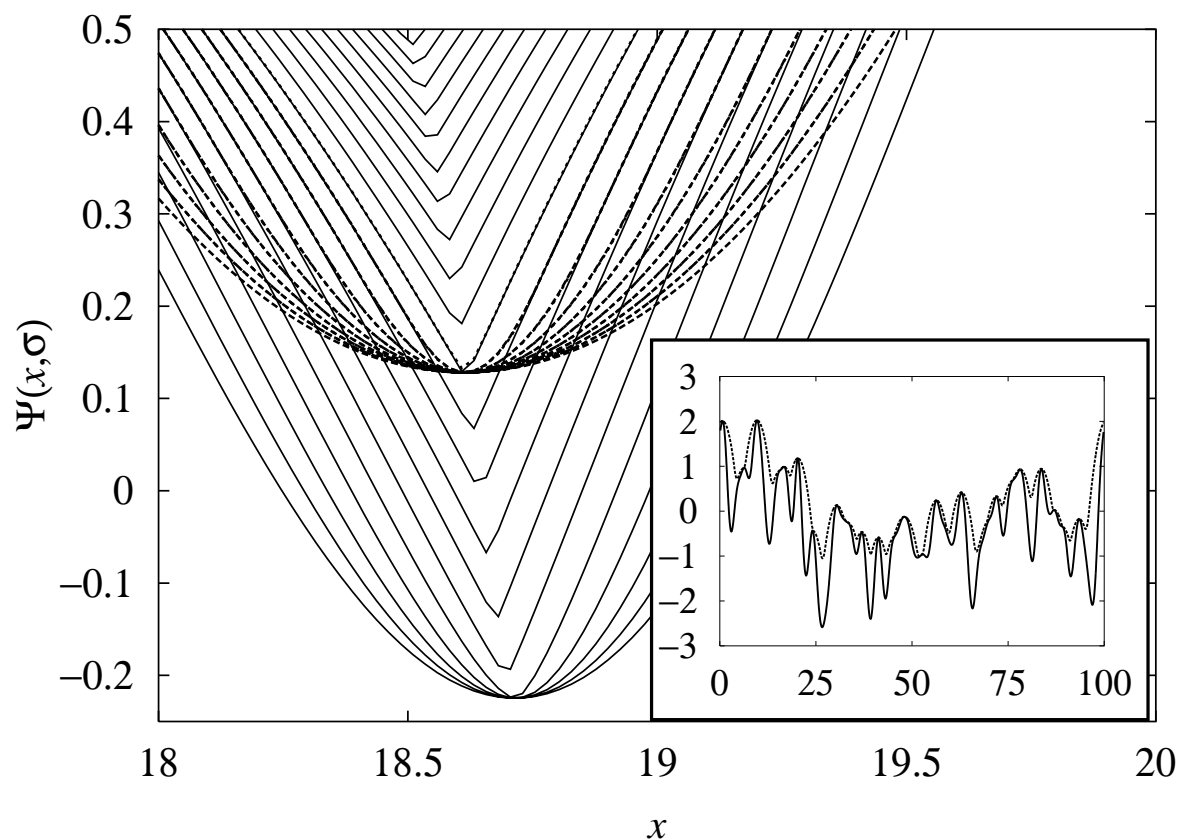


Figure 2, Sethna *et al.*

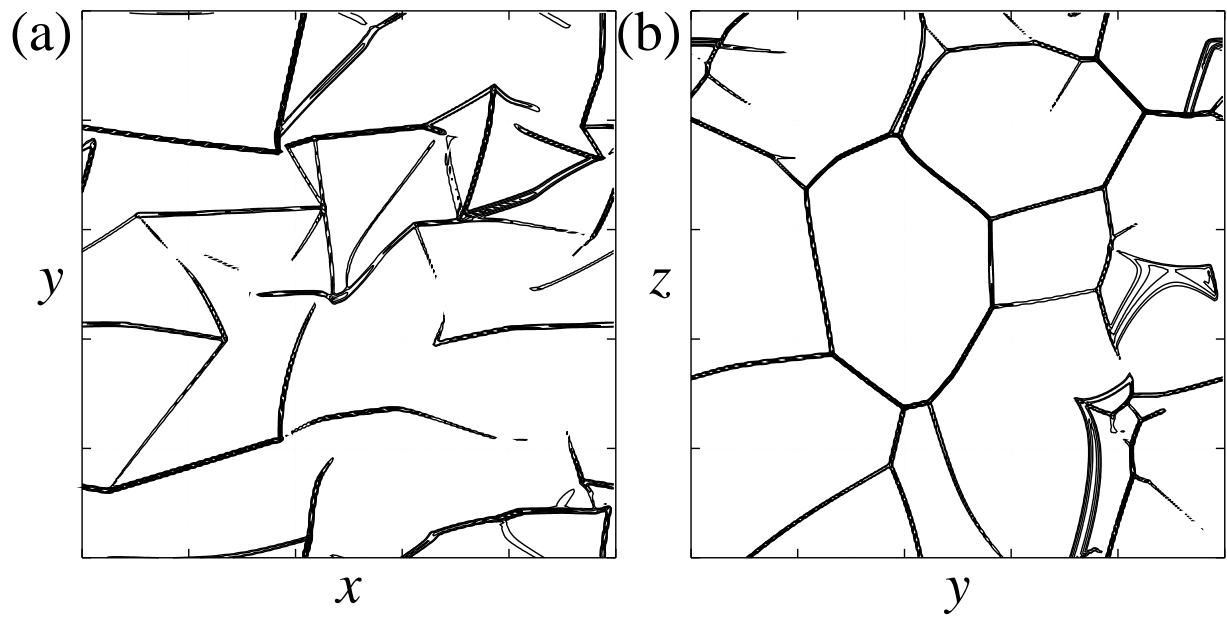


Figure 3, Sethna *et al.*

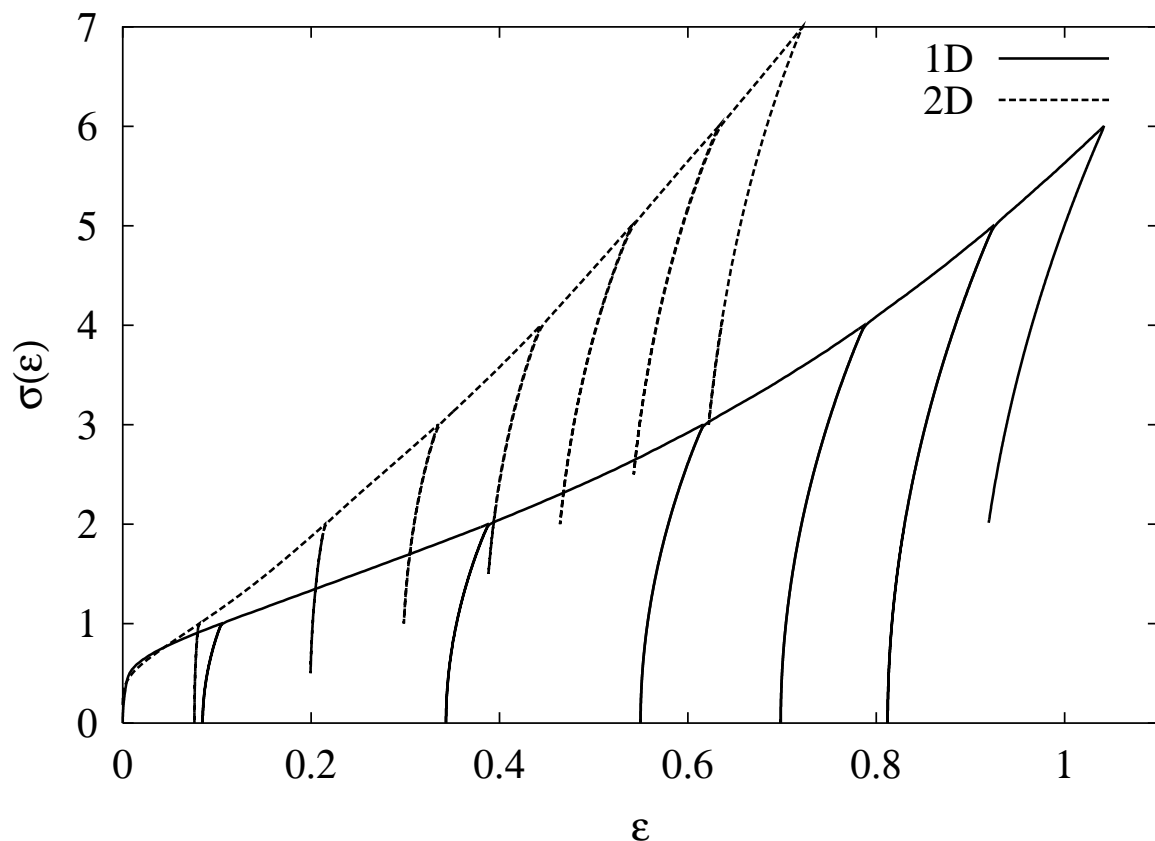


Figure 4, Sethna *et al.*

